BIOCHEMISTRY
including biophysical chemistry & molecular biology

Article

pubs.acs.org/biochemistry

Aspartate Embedding Depth Affects pHLIP's Insertion pK_a

Justin Fendos,[‡] Francisco N. Barrera,[†] and Donald M. Engelman*[,†]

[†]Department of Molecular Biophysics and Biochemistry, Yale University, New Haven, Connecticut 06520, United States
[‡]Department of Biotechnology, Dongseo University, Busan 617-716, South Korea

Supporting Information

ABSTRACT: We have used the *pH low insertion peptide* (pHLIP) family to study the role of aspartate embedding depth in pH-dependent transmembrane peptide insertion. pHLIP binds to the surface of a lipid bilayer as a largely unstructured monomer at neutral pH. When the pH is lowered, pHLIP inserts spontaneously across the membrane as a spanning α-helix. pHLIP insertion is reversible when the pH is adjusted back to a neutral value. One of the critical events facilitating pHLIP insertion is the protonation of aspartates in the spanning domain of the peptide: the negative side chains of these residues convert to uncharged, polar forms, facilitating insertion by altering the hydrophobicity of the spanning domain. To examine this protonation mechanism further, we created pHLIP sequence variants in which the two spanning aspartates (D14 and D25) were moved up or down in the sequence. We hypothesized that the aspartate depth in the inserted state would directly affect the proton affinity of the acidic side chains, altering the pK_a of pH-dependent insertion. To this end, we also mutated the arginine at position 11 to determine whether arginine snorkeling modulates the insertion pK_a by affecting the aspartate depth. Our results indicate that both types of mutations change the insertion pK_a, supporting the idea that the aspartate depth is a participating parameter in determining the pH dependence. We also show that pHLIP's resistance to aggregation can be altered with our mutations, identifying a new criterion for improving the performance of pHLIP *in vivo* when targeting acidic disease tissues such as cancer and inflammation.

We have shown previously that the C helix of bacteriorhodopsin, called *pH low insertion peptide* (pHLIP), is capable of targeting acidic tissues and inserting into cell plasma membranes both *in vitro* and *in vivo*.[1−4] This is significant because localized extracellular acidity is a hallmark of many diseases, including cancer, inflammation, and ischemia.[5] When conjugated to positron emission tomography (PET)[6] and fluorescent[1,4] probes, pHLIP is able to target mouse tumors *in vivo* with high specificity, demonstrating potential for therapeutic use in cancer diagnosis.[7] pHLIP may also function as a drug delivery platform, translocating small cell-impermeable cargo molecules such as organic dyes,[2] cyclic peptides,[3,8] and peptide nucleic acids (PNAs) into the cytoplasm of cultured cells.[2] Importantly, pHLIP does not exhibit obvious toxicity in cells or mice,[1,4] further promoting its therapeutic potential.

pHLIP is monomeric at low concentrations[9] and adopts a largely unstructured conformation in neutral pH aqueous environments,[10,11] a condition we call state I. When lipid vesicles are added at neutral pH, pHLIP is partitioned favorably to the lipid surface with a ΔG of 6−7 kcal/mol.[12] In this surface-attached state, called state II, pHLIP remains largely unstructured[10,13] and is hardly distinguishable from state I by circular dichroism (CD). However, when the pH is lowered, pHLIP inserts into membranes as a membrane-spanning α-helix,[9,14] adopting the state III conformation. This insertion is fully reversible, with the peptide's C-terminus translocated across the membrane upon insertion.[3,14] The pK_a of insertion into POPC liposomes is 6.0.[10,13]

The pHLIP primary sequence contains several acidic residues (Table 1). At neutral pH, the combined negative charge of these residues, together with the free carboxyl at the C-terminus, produces a large energy barrier that prevents pHLIP insertion at neutral pH. The energetic cost of partitioning a single aspartate from water into octanol on the Wimley−White scale[15] is 3.6 kcal/mol for the unprotonated form but only 0.4 kcal/mol for the

Table 1. Primary Sequence of the pHLIP Single-Mutation Variants Used in This Study[a]

Name.	Sequence.
WT pHLIP	GGEQNPIYWA**R**YA**D**WLFTTPLLLL**D**LALLVDADEGTCG
R11Q	GGEQNPIYWA**Q**YADWLFTTPLLLLDLALLVDADEGTCG
D14Up	GGEQNPIYWARY**DA**WLFTTPLLLLDLALLVDADEGTCG
D14Down	GGEQNPIYWARYA**WD**LFTTPLLLLDLALLVDADEGTCG
D25Up	GGEQNPIYWARYADWLFTTPLLL**DL**LALLVDADEGTCG
D25Down	GGEQNPIYWARYADWLFTTPLLLL**LD**ALLVDADEGTCG

[a]Blue letters indicate the arginine at position 11 and the aspartic acids at positions 14 and 25 that have been mutated. Red letters indicate the experimental alterations.

Received: February 27, 2013
Revised: May 28, 2013
Published: May 30, 2013

protonated form.[16] It is this conversion that allows pHLIP insertion at low pH.[1,9]

Previous work has shown that the number of aspartic residues in the inserting portion of the peptide has an effect on pHLIP's insertion pK_a.[13,17] In the present work, we examine whether the *position* of the two spanning aspartates at positions 14 and 25 play a role as well. Local water availability around acidic residues is known to play an important role in determining the proton affinity of the side chains.[18] We were therefore interested in determining whether changes in aspartate position would give rise to changes in the insertion pK_a, indicating that the embedding depth in the inserted state (state III) affects pHLIP's pH sensitivity by modulating its proton affinity. Along related lines, we were interested in seeing whether mutation of the arginine at position 11 would affect the insertion pK_a, since changes could indicate that arginine snorkeling also participates in regulating the aspartate embedding depth in state III.

MATERIALS AND METHODS

Peptide Synthesis. Peptides were made using the 9-fluorenylmethyloxycarbonyl solid-phase synthesis service provided by the W. M. Keck Foundation Resource at Yale University (New Haven, CT). After synthesis, the peptides were purified by reversed-phase high-performance liquid chromatography (HPLC) on a C18 column using a water/acetonitrile gradient. The purity was determined by matrix-assisted laser desorption ionization time of flight (MALDI-TOF) mass spectrometry, and the quantity of peptide was determined by absorbance spectroscopy using a molar extinction coefficient of 13 940 M^{-1} cm^{-1}.

Peptides were synthesized with a single cysteine residue at the C-terminus for use in disulfide-bond cargo attachment (see Table 1 for the list of variants). To work out ionic strength conditions that did not promote dimerization or aggregation, different amounts of wild-type (WT) pHLIP-cys were incubated in phosphate buffer for varying periods of time. The resulting samples were assayed for dimer by both HPLC (data not shown) and tryptophan fluorescence (TF) (see Figure 1A). Both WT pHLIP disulfide dimerization (reagent-assisted) and aggregation (at high peptide concentrations) have been shown to cause a quenching blue shift detectable by fluorescence. These experiments yielded HPLC and TF data in agreement with each other, showing that very low concentrations of WT pHLIP ($\leq$7 μM) do not dimerize or aggregate significantly for very long periods of time (>12 h) in 5, 10, and 20 mM phosphate buffer. Because of the agreement between assays and the fact that HPLC requires more material, only TF was used to assess aggregation/dimerization in the pHLIP variants.

Peptide Preparation. The final peptide preparation procedure used for this work involved resuspension of lyophilized peptide flakes in 5 mM phosphate buffer (pH 8.0) to create peptide stock solutions with concentrations of 20−30 μM. These stock solutions were used within 1 h to avoid aggregation.

Liposome Preparation. The desired amount of chloroform-dissolved 1-palmitoyl-2-oleoyl-*sn*-glycero-3-phosphocholine (POPC) lipid from Avanti Polar Lipids was dried in a glass tube, first with nitrogen gas and then under vacuum overnight. The dried lipid was resuspended in 5 mM phosphate buffer (pH 8.0) to achieve the desired stock concentration, and the suspension was mixed thoroughly by vortexing. To make POPC liposomes, the resuspended lipids were extruded through one polycarbonate membrane with a pore size of 0.1 μm (Nuclepore, Whatman). This extrusion was performed using a "Mini-Extruder" syringe system. Depending on the lipid concentration, 15−30 extrusion steps were performed to obtain a homogeneous population of large unilamellar vesicles (LUVs). HPLC was used once when establishing the procedure to determine a homogeneous vesicle population.

Insertion Assay by Tryptophan Fluorescence. Peptide and POPC vesicle stock solutions were prepared as described above, diluted, and incubated together at a peptide:lipid molar ratio of 1:300 for 1 h. The dilution was in 5 mM phosphate buffer (pH 8.0), reaching a final peptide concentration of 10 μM. This incubation was performed to give the peptide ample time to complete partitioning to the liposome surface (the "parking step").

After incubation, the peptide/vesicle stock solution was further diluted to create a panel of samples, each at a final peptide concentration of 1.5 μM. The pH was adjusted in this final dilution using a panel of 250 mM phosphate stock buffers, each titrated to a different pH. Each sample in the panel was mixed with a fixed aliquot of stock buffer to adjust the pH to a unique value in the range from 3.5 to 8.0 while maintaining constant buffer concentration. To provide adequate coverage of the pH range, 20−30 samples were made. The final phosphate concentration was 20 mM. After a 10−15 min incubation to allow the pH titration to take effect, the emission spectrum of each sample was measured at room temperature with excitation at 295 nm using a SLM-Aminco 8000C spectrofluorimeter. Appropriate liposome-only blanks were subtracted in all cases.

For the determination of the spectral maxima, a fitting procedure using the root-mean-square criterion (SIMS) was applied to the emission curves. This procedure fits the experimental spectra to a series of log-normal components.[19] The spectral maxima thus obtained for the samples in the pH range were plotted and analyzed according to a sigmoidal fit[20] as follows:

$$F = \frac{F_a + F_b 10^{m(\mathrm{pH}-\mathrm{p}K_a)}}{1 + 10^{m(\mathrm{pH}-\mathrm{p}K_a)}} \quad (1)$$

where m is the slope of the sigmoidal transition, $F_a = (f_A + S_A \cdot \mathrm{pH})$, and $F_b = (f_B + S_B \cdot \mathrm{pH})$. In the expressions for F_a and F_b, f_A and f_B are the spectral maxima for the acid and basic forms, respectively, and S_A and S_B are the slopes of the acid and base baselines, respectively. The midpoint of the sigmoid gives the pK_a of insertion. Nonlinear least-squares fitting was carried out using the Origin software (OriginLab, Northampton, MA).

Insertion Assay by Circular Dichroism. Samples were prepared as in the TF experiments but with a final peptide:lipid molar ratio of 1:200 and a final peptide concentration of 5 μM. This was done both to enhance the signal from the peptide and to reduce light scattering from the lipids. CD spectra were recorded on a Jasco J-810 spectropolarimeter interfaced with a Peltier temperature system. Spectra were recorded at room temperature using a 2 mm cuvette. The scan rate was 100 nm/min, and 30 scans were averaged for each sample. Raw data were converted to mean residue ellipticities $[\theta]$ (in deg cm^2 $dmol^{-1}$) as follows:[21]

$$[\theta] = \frac{\theta_{obs}}{10lcn} \quad (2)$$

where θ_{obs} is the measured ellipticity (in deg), l is the cell path length (in cm), c is the protein concentration (in dmol/cm^3), and n is the number of amino acids per molecule. Appropriate lipid blanks were subtracted in all cases.

dx.doi.org/10.1021/bi400252k | *Biochemistry* 2013, 52, 4595−4604

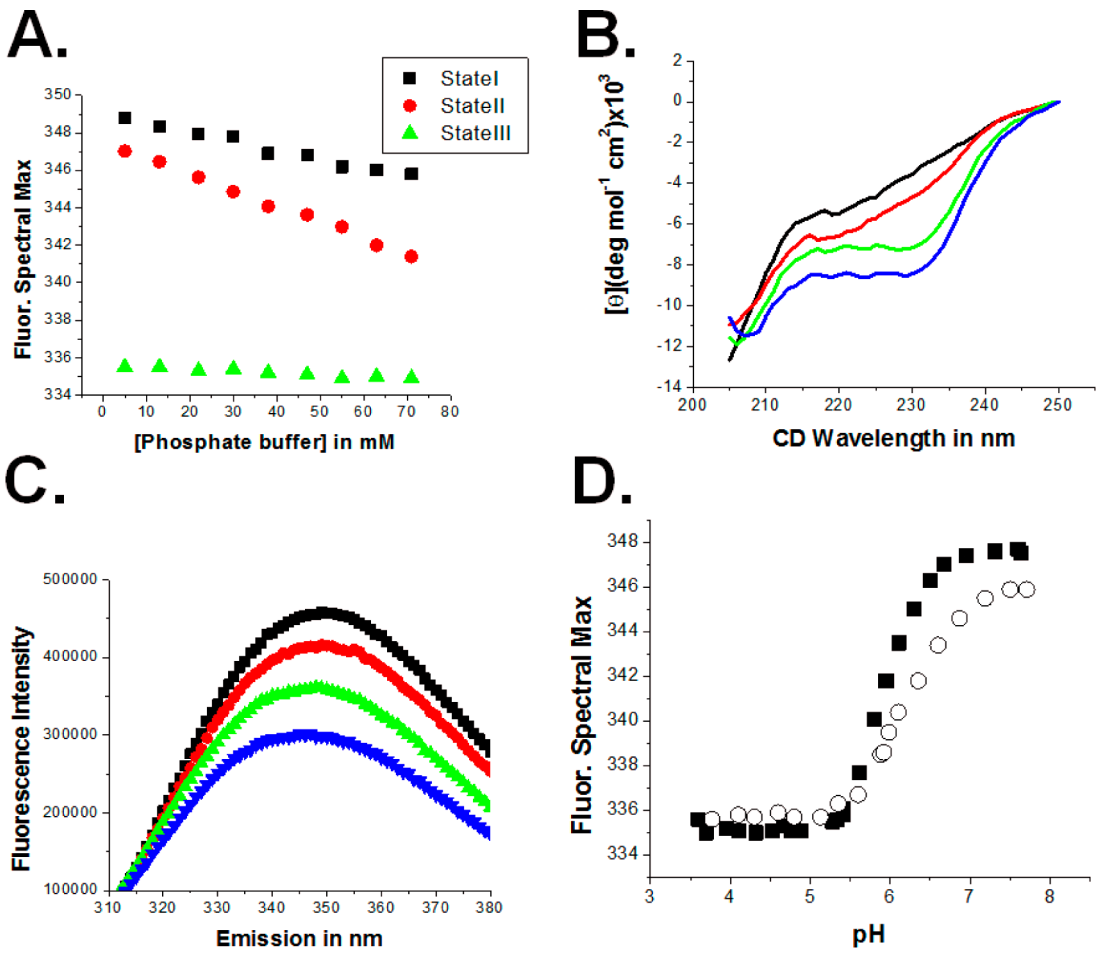

Figure 1. Ionic strength affects the three states of pHLIP. (A) Increasing the phosphate concentration causes blue shifts in the tryptophan fluorescence (TF) of states I and II. Conditions: 1.5 μM WT pHLIP, 1:300 peptide:lipid ratio. (B) Increasing [phosphate] increases the helicity of state I, presumably by driving aggregation: black, 5 mM phosphate; red, 25 mM; green, 50 mM; blue, 75 mM. Conditions: 5 μM pHLIP, pH 7.20 ± 0.09. (C) Increasing [phosphate] results in loss of state I TF intensity, indicating tryptophan quenching or peptide loss from solution, both consistent with aggregation: black, 5 mM phosphate; red, 20 mM; green, 40 mM; blue, 80 mM. (D) The properties of a pH-dependent insertion sigmoid change with [phosphate]. Shown are fluorescence spectral maxima at [phosphate] = 20 mM (■) and 55 mM (○). The insertion pK_a's were 5.95 ± 0.06 at 20 mM and 6.18 ± 0.09 at 55 mM.

State I Aggregation Experiments. Peptide stock solutions for ionic and pH aggregation were prepared as above. In ionic strength aggregation experiments, the peptide stock solution was diluted into a series of samples adjusted to different final ionic strengths using various volumes of 250 mM phosphate buffer (pH 7.4). For each sample, the final peptide concentration was 3 μM and the final pH was 7.44 ± 0.10. Linear fits were made using Excel.

For pH aggregation experiments, the peptide stock solution was diluted into a series of samples adjusted to different pH using a panel of stock 250 mM phosphate buffers. The resulting series had a peptide concentration of 3 μM, a phosphate buffer concentration of 10 mM, and a final pH between 4 and 8. Midpoints were determined using the same fitting procedure as above (eq 1).

After preparation, each set of samples was incubated for 10 min before fluorescence measurements at room temperature were performed as described above. Time was an important variable for the output of these experiments, so the incubation time had to be controlled. For ionic strength aggregation, samples were always measured from lower to higher ionic strength, while pH variation samples were measured from high to low pH.

Reversibility Experiments. Peptide and lipid stock solutions were prepared as described above and used to make peptide/lipid mixtures in 5 mM phosphate buffer (pH 8.0) as for the TF experiments. The peptide:lipid ratio was 1:300, and the peptide concentration was 5 μM. After incubation for 1 h to "park" the peptides, samples were read once by fluorescence before the pH was adjusted to a value of 4.11 ± 0.09 using a set quantity of concentrated HCl. The samples were read again by fluorescence over the course of 10 min before a small aliquot (<3 μL) of concentrated sodium hydroxide was added to return the pH to 7.69 ± 0.07. The TF was again read over a 10 min interval. Spectral maxima were determined as described above.

RESULTS

Selection of Single-Mutant Variants. It has been shown previously that the proton affinity of acidic side chains depends on the local water environment[18] in such a way that a more hydrophobic environment results in higher affinity. This mechanism depends on the fact that there are fewer water molecules to solvate the acidic proton once it is bound to the side chain.

dx.doi.org/10.1021/bi400252k | *Biochemistry* 2013, 52, 4595−4604

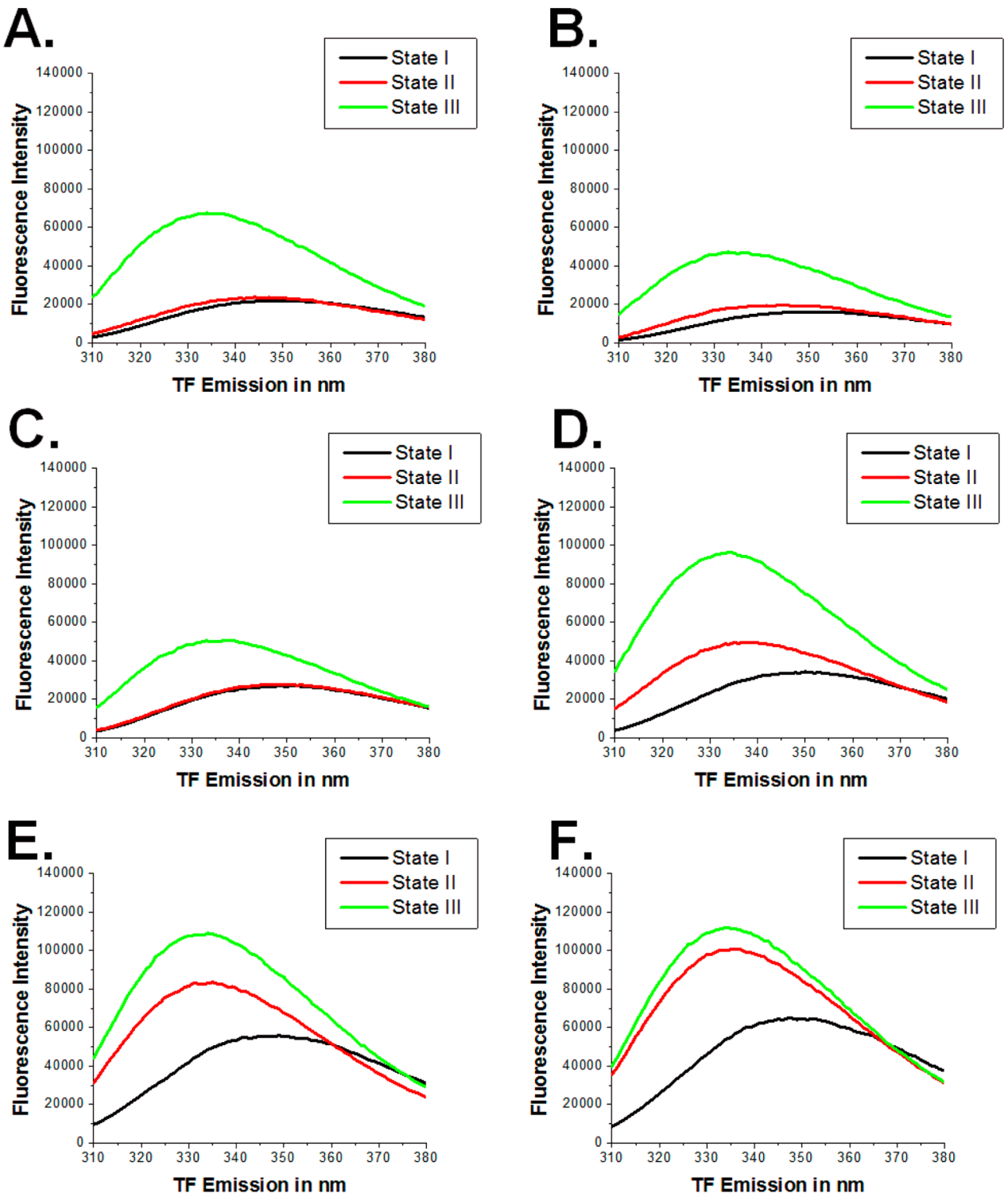

Figure 2. Fluorescence spectra of the three states of (A) WT pHLIP, (B) R11Q, (C) D14Up, (D) D14Down, (E) D25Up, and (F) D25Down. R11Q and D14Up exhibit a clear state II to state III transition comparable to that for the WT (also see Figure S5 in the Supporting Information). D14Down exhibits some II → III transition, while D25Up and D25Down exhibit aberrant transitions. In all cases, 1.5 μM peptide and 0.45 mM POPC were used (peptide:lipid ratio = 1:300). For states I and II, pH = 7.20 ± 0.10; for state III, pH = 4.25 ± 0.08.

In the context of inserted pHLIP (state III), it is conceivable that the embedding depth of the spanning aspartates at positions 14 and 25 in state III could play a role in determining the off rate of the acidic protons. Previous work[22] has shown that the water profile inside a lipid bilayer is uneven, with hydration decreasing precipitously with deeper penetration. This lack of water could mean that the side-chain proton affinity is higher at locations deeper in the membrane.

The most direct way of examining embedding depth as a parameter is by directly changing the position of the aspartate residues in the spanning domain. This is the first of two strategies we employed. The second, more indirect strategy involved

dx.doi.org/10.1021/bi400252k | *Biochemistry* 2013, 52, 4595−4604

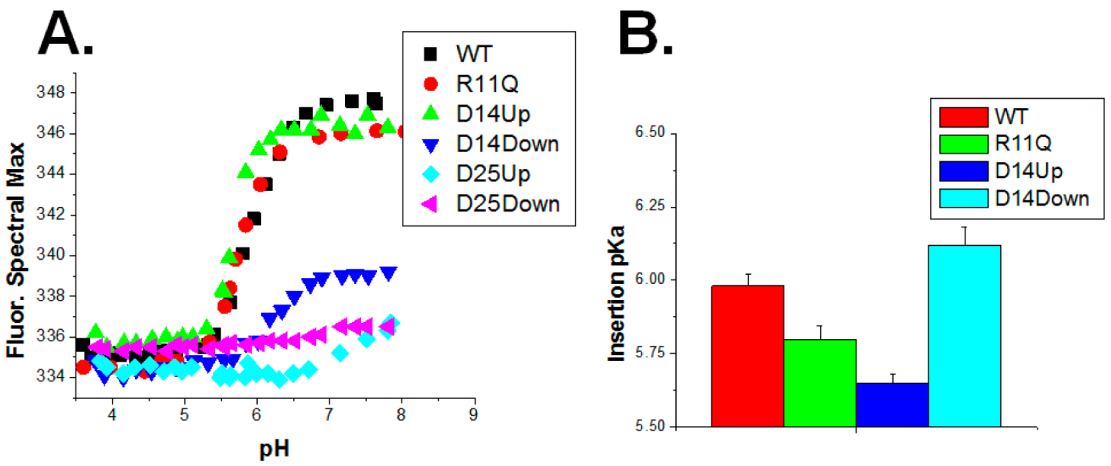

Figure 3. The variants have different insertion pK_a values. (A) TF spectral maxima plotted vs pH. Conditions: 1.5 μM peptide, peptide:lipid ratio = 1:300. (B) The insertion pK_a values are different (average from $n = 4$). Values for D25Up and D25Down were not included because they did not exhibit an obvious sigmoidal transition in (A).

mutating the arginine at position 11 (R11). It has been reported previously[23,24] that arginines can have strong "snorkeling" effects that buoy regions of a transmembrane peptide closer to the interfacial surface. An open question for pHLIP was whether or not R11 plays such a role. To examine this possibility, we mutated R11 to a glutamine (Table 1). Glutamine was selected because its hydrophobicity is most similar to that of arginine on the Wimley–White scale.

Defining the Experimental Conditions with WT pHLIP. To ensure experimental consistency, we defined a specific set of conditions with WT pHLIP. Previous work[2,10] had established pH, peptide concentration, and peptide:lipid ratio guidelines for performing pHLIP experiments. However, one parameter that was not previously well-established was ionic strength. Previous protocols involved dialyzing pHLIP into solutions of physiological ionic strength.[24] However, it has been found that exposure to high ionic strength results in both a fluorescence blue shift and a loss of TF intensity (Figure 1A,C). This is consistent with previous observations for WT pHLIP in which aggregation or dimerization of the peptide at high concentration (as confirmed by HPLC) produced an identical effect on the fluorescence (unpublished data). Because of these observations, we devised a peptide preparation protocol with a very low peptide concentration and low ionic strength to prevent aggregation/dimerization. Both restrictions alleviated the problem significantly when using WT peptide (Figure 1 and data not shown).

Interestingly, it was found that ionic strength had an effect on the spectral maxima of pHLIP samples in state II (Figure 1A) as well as state I. This suggested that increasing ionic strength promotes partitioning of pHLIP from the aqueous environment to the membrane surface. This would be consistent with a mechanism in which soluble charge drives hydrophobic components away from solution, which should promote membrane partitioning and aggregation similarly. It was therefore not surprising to find that different ionic conditions resulted in slightly different insertion pK_a values as well (Figure 1D), since state II partitioning is an integral part of insertion. These results are significant when considering future use of WT pHLIP and pHLIP variants *in vivo*, since the ionic strength of blood is considerably higher than these optimized values *in vitro*.

Tryptophan Fluorescence. In addition to indirect assessment of aggregation, TF can be used to monitor the local environment of tryptophan residues at positions 9 and 15 (Figure 2A), giving direct information about pHLIP's interactions with membranes through an assessment of the local hydrophobic environment. To test our variants for membrane interactions, we performed insertion experiments into POPC liposomes using low-ionic-strength conditions. Much to our surprise, not every peptide exhibited three distinguishable states like WT. The D25Up and D25Down variants, for instance, exhibited state II behavior that looked more similar to WT state III (Figure 2E,F). This indicated the possibility the peptides were either inserting spontaneously or aggregating on the membrane surface. D14Down also exhibited this aberrant state II behavior but to a lesser extent (Figure 2D). As the sequence variations from WT pHLIP were very small and the overall hydrophobicities were identical, it seems most likely that the membrane surface induced the aggregation since there would seem to be no other element in the system to overcome the large energy barrier for insertion.

From plots of the TF spectral maxima versus pH in the presence of liposomes, it was possible to reconstruct the II → III transition as a sigmoid for WT pHLIP (Figure 3A). Using this method, we could mathematically determine the midpoint, which is equal to the pK_a of insertion. This pK_a defines the acidic proton concentration at which half of the peptide molecules are inserted into the membrane.[10] In agreement with our hypothesis of D25Up and D25Down aggregation, no insertion pK_a was obtained for these peptides (Figure 3B). The remaining peptides, with the exception of D14Down, all had insertion pK_a values lower than that of WT pHLIP.

Circular Dichroism. CD is used to examine the secondary structure of peptides. We employed it to monitor the helical transition of state II to state III (Figure 4A). As in the TF measurements, D25Up and D25Down exhibited altered state II behavior, showing more secondary structure than the WT (Figure 4E,F). In addition, their states I seemed to have more helicity, another strong indicator of aggregation. D14Down similarly exhibited state I and state II behavior very different from those for the WT but not as different as for D25Up and D25Down (Figure 4D), suggesting that D14Down aggregates only partially. All of the other variants showed behavior similar that of the WT. Some effort was put into trying to reconstruct insertion pK_a values from the CD plots, but the variability of the data from experiment to experiment proved to be a deterrent (data not shown).

dx.doi.org/10.1021/bi400252k | *Biochemistry* 2013, 52, 4595–4604

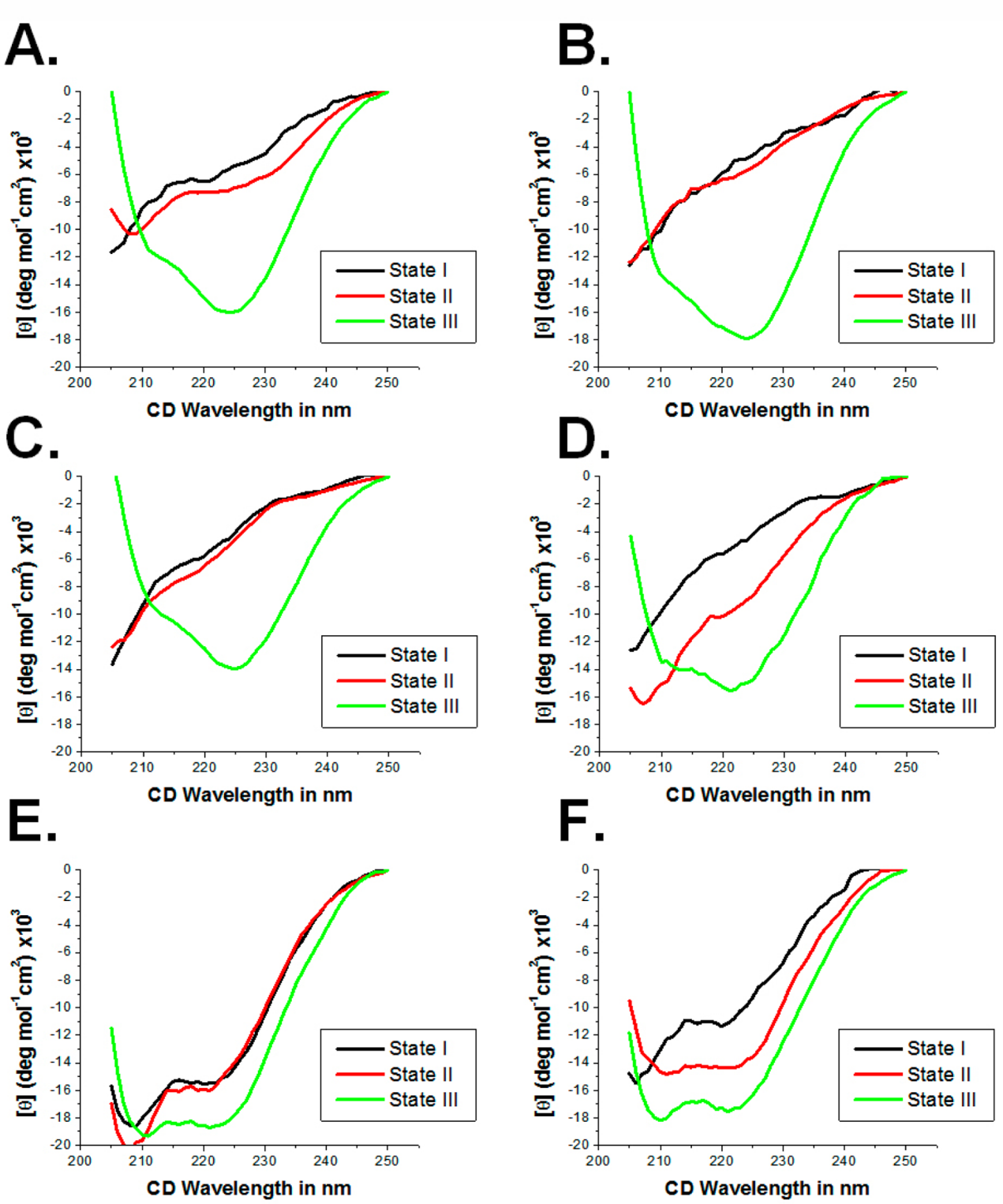

Figure 4. CD spectra of the three states of (A) WT pHLIP, (B) R11Q, (C) D14Up, (D) D14Down, (E) D25Up, and (F) D25Down. R11Q and D14Up exhibited obvious helicity increases in going from state II to state III that mimicked those of the WT, in agreement with the TF results (Figure 2). D14Down exhibited a similar but not identical helical transition, while D25Up and D25Down exhibited aberrant helicity in both states I and II (also see Figure S5 in the Supporting Information). Conditions: 5 μM peptide, peptide:lipid ratio = 1:200, pH = 7.22 $\pm$ 0.09 for states I and II and 4.27 $\pm$ 0.08 for state III.

Insertion Reversibility. An important criterion for true pHLIP insertion is reversibility. WT pHLIP insertion can be reversed by raising the acidic pH of a state III sample to a value above 7 (Figure S1A in the Supporting Information). To examine reversibility in our variants, the fluorescence from peptide/POPC samples was recorded once at pH 7.8, recorded again over a 10 min time interval after the pH was adjusted to a low value (4.11 $\pm$ 0.11), and recorded again over a second 10 min

dx.doi.org/10.1021/bi400252k | *Biochemistry* 2013, 52, 4595−4604

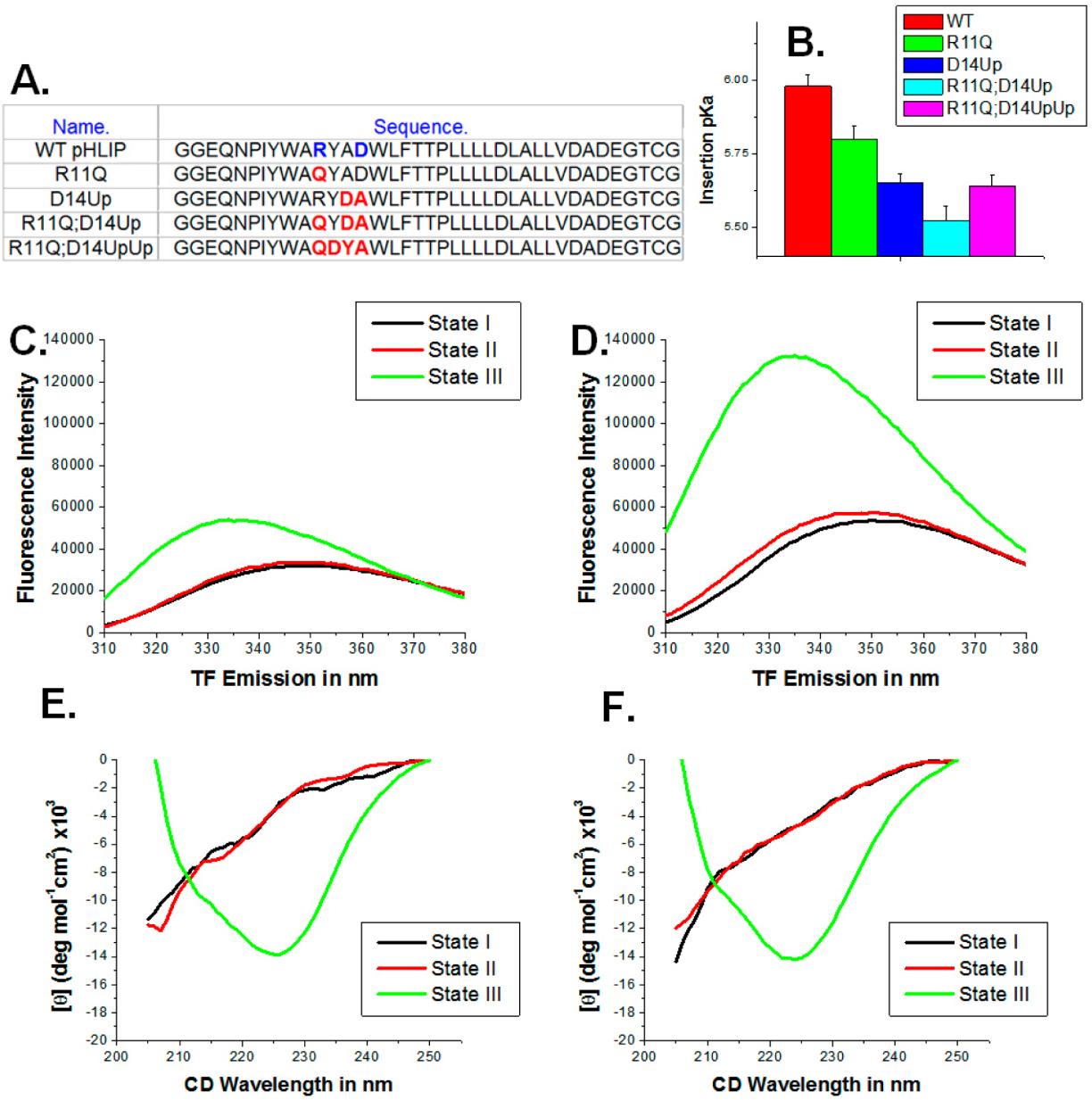

Figure 5. (A) Sequences of the two double variants used (R11Q;D14Up and R11Q;D14UpUp), the parent sequences (R11Q and D14Up), and WT pHLIP. (B) Comparison of the insertion pK_a's of the double variants with those of the parent variants and WT pHLIP ($n = 3$). (C, D) TF spectra of (C) R11Q;D14Up and (D) R11Q;D14UpUp under the three state conditions, showing that the double variants exhibit insertion behavior much like that of the WT. Conditions: 1.5 μM peptide, peptide:lipid ratio = 1:300. (E, F) CD spectra of (E) R11Q;D14Up and (F) R11Q;D14UpUp under the three state conditions, showing that the double variants exhibit behavior much like that of the WT: a clear helical transition between states II and III. Conditions: 5 μM peptide, peptide:lipid ratio = 1:200. Also see Figure S5 in the Supporting Information).

interval after the pH was returned to a basic value (7.69 ± 0.10). As might be anticipated from the other experiments, R11Q and D14Up exhibited clear reversibility, much like the WT, and D14Down exhibited some reversibility, consistent with the idea it may be only partially aggregated (Figure S1A). D25Up and D25Down exhibited no reversibility, again consistent with aggregation (Figure S1B).

Aggregation by Ionic Strength Challenge. Since pHLIP's aggregation is intimately related to ionic strength (Figure 1A), we were curious to see how the variants would respond to an ionic strength challenge. For use *in vivo*, pHLIP–fluorophore conjugates are typically injected into mice at very high concentrations (30–100 μM). Since body fluids have moderately high ionic strength (similar to phosphate buffers at 50–55 mM), it remains questionable how much of the injected peptide is actually in a functional, monomeric form. It is possible that serum albumin and other components of the blood help to dissociate aggregates, but it is also possible that pHLIP aggregates are permanent, significantly reducing the available pool of functional monomers. From the standpoint of clinical use, it is therefore desirable to engineer peptides that have as little aggregation as possible while maintaining pH-dependent insertion.

By plotting the spectral maxima of peptide samples across a phosphate buffer concentration range, we were able to observe three types of behavior (Figure S2A in the Supporting

dx.doi.org/10.1021/bi400252k | *Biochemistry* 2013, 52, 4595–4604

Information). For D25Up and D25Down, the spectral maxima blue-shifted rapidly before saturating. The WT and D14Down also exhibited saturation behavior, but this occurred more gradually and at higher ionic strengths. The spectral maxima of the remaining peptides behaved linearly. From these plots, we fit an initial slope to each (Figure S2B) and used this value as an indication of how quickly that peptide responds to ionic challenge. Interestingly, R11Q aggregated less than WT pHLIP, suggesting that it may be more amenable for use *in vivo* while still maintaining pH-dependent insertion. In addition to aggregating less in response to ionic strength challenge, R11Q did not saturate in the ionic strength range examined (Figure S2A).

Aggregation by pH Challenge. Although pH challenge is not as physiologically relevant as ionic strength challenge, we were also interested in seeing how the variants responded to pH changes. We knew from previous unpublished work that pHLIP readily aggregates in solution below pH 6.0 in the absence of lipids. By plotting the spectral maxima across a pH range, we found that pH challenge resulted in sigmoidal transitions much like those observed for lipid insertion. Taking the midpoint of each sigmoid as the "pH aggregation pK_a", we found that the pattern of pH dependence was the same as for ionic challenge: D14Down, D25Up, and D25Down aggregated at a higher pH than the WT, while R11Q and D14Up responded at a lower pH (Figure S3A in the Supporting Information). Interestingly, when these pH-dependent aggregation midpoints were plotted alongside the insertion pK_a values, we found that each pH aggregation pK_a was lower than the corresponding insertion pK_a (Figure S3B). We speculate this may be a characteristic requirement for peptides that undergo a true pHLIP-like state II to state III transition: they must have higher pH-dependent affinities for lipids than for themselves.

R11Q;D14Up Double Variant. From the above data, it might be hypothesized that a pHLIP double variant with both R11Q and D14Up might have a combination of desired properties: a lower insertion pK_a than the WT and less aggregation. To test this notion, we created the R11Q;D14Up double variant (Figure 5A) and found it to have a lower insertion pK_a than the two single variants (Figure 5B and Figure S6 in the Supporting Information) and less aggregation when challenged with ionic strength (Figure S4A in the Supporting Information). The pH-dependent aggregation (Figure S4B) was not obviously different from that of R11Q but was lower than that of D14Up. This variant still exhibited clear, reversible insertion (Figure S4C) as determined by TF (Figure 5C) and CD (Figure 5E). We suggest that this variant may prove useful for *in vivo* applications for the reasons discussed above.

R11Q;D14UpUp Double Variant. To explore further the idea of aspartic depth in state III as a parameter for controlling the insertion pK_a, we also created the R11Q;D14UpUp variant. In this variant, the R11Q mutation was combined with a new mutation in which the aspartate at position 14 was moved up two units in the primary sequence (Figure 5A). If aspartate depth is directly responsible for the lower insertion pK_a of the R11Q;D14Up variant, the R11Q;D14UpUp variant would be expected to have an even lower pK_a.

Interestingly, a lower pK_a was not observed. Although the TF and CD spectra indicated that this peptide exhibited proper pH-dependent insertion (Figure 5D,F), R11Q;D14UpUp had an insertion pK_a indistinguishable from that of D14Up (Figures 5B and S6) despite exhibiting insertion reversibility (Figure S4C) and aggregation behavior very similar to that of R11Q;D14Up (Figure S4A,B).

DISCUSSION

The two main outcomes from this study are (1) further understanding of the elements of pHLIP's primary sequence that control its aggregation properties and insertion pK_a and (2) the possible design of a peptide with improved properties for use *in vivo*. For the latter, reduced aggregation tendency and a lower insertion pK_a are likely to be desirable properties. Reduced aggregation tendency may result in a larger pool of conjugated peptide that is available for targeting, while a lower insertion pK_a may enhance targeting by increasing the sensitivity to local acidity, thereby reducing off-target localization. This reduction is especially important since the pH difference between normal tissue and tumor tissue is often quite small (typically 0.2−0.5 pH units depending on the experimental method and tissue type).[5]

As the above results show, the D14Up, R11Q, R11Q;D14Up, and R11Q;D14UpUp peptides exhibit both a lower insertion pK_a than the WT and superior resistance to aggregation. From a pure materials standpoint, we offer R11Q;D14Up as the peptide with the greatest potential for improved *in vivo* use. Although the potential for enhanced localization *in vivo* was not explored in this study, future work should examine the possibility.

In the aberrant cases of D14Down, D25Down, and D25Up, a direct assessment of the cause of the different behavior relative to the WT is problematic. Given the strong blue shift of the TF for all three peptides in state II, we speculate that they most likely may aggregate at the membrane surface. It is very interesting to note how drastically the properties of the peptide can change even with a single one-position modification in sequence order. This offers the tantalizing possibility that D25 may be part of a critical interaction interface for the peptide in state II that can promote aggregation when D25 is moved out of the way. This is particularly interesting since previous work in which D25 was mutated to histidine showed only very mild changes in behavior.[13]

Insertion pK_a Changes. One question we posed was whether the depth of the spanning aspartates plays a role in changing the insertion pK_a, as might be expected from the changing water profile in a bilayer.[25] The data provided some support for this idea: when D14 was moved up, the insertion pK_a decreased, and when D14 was moved down (ignoring the partial aggregation), the insertion pK_a increased, just as our hypothesis predicted.

R11Q's contribution is unclear because we have no way of knowing for sure how the mutation changes the relative depth of the spanning aspartates. However, the pK_a for R11Q;D14UpUp goes against the model. In R11Q;D14UpUp, aspartate 14 was moved up two positions and yet the pK_a increased. There are several possible explanations for this, two of which we will discuss. First, it is possible that the model is wrong. A second, more interesting possibility is that an aspartic residue at position 12 (D14UpUp) may be too high in the sequence to remain in the hydrophobic core when the peptide is in the inserted state. If this is the case, that aspartate may no longer have to retain its acidic proton to keep the peptide stably inserted. In effect, an aspartate at position 12 may no longer participate (or may participate to a lesser degree) in determining the insertion pK_a.

This idea of insertion frame prompted us to consider the question of what might be the most favorable portion of pHLIP to reside in the hydrophobic core. Using previous results[26] to extrapolate the approximate thickness of a POPC hydrophobic

core (from the second acyl chain carbon of one monolayer to the second acyl carbon of the other), we found that a pure α-helix segment of about 18 residues is sufficient to span the extrapolated core fully. Using the MPEx membrane domain predictor,[16] we determined what part of WT pHLIP might be most likely to reside in a membrane-spanning domain of this length and found that the most favorable sequence is the following underlined portion of WT pHLIP: GGEQNPIYWARYADWLFTTPLLLLDLALLVDADEGTCG. We were surprised by this prediction because it does not contain the arginine at position 11, even though mutation of R11 affects the insertion pK_a. This offers the possible suggestion that R11 may have more of a role in state II embedding and impart its effects on the insertion pK_a indirectly without being a component of the spanning domain.

It is of course essential to note that any algorithm such as MPEx is inherently imperfect because the tilt of the inserted helix, the exact number and identity of the inserted residues, and the rotational conformations of the inserted side chains is composed of a grand ensemble of states no algorithm can hope to convey. Nevertheless, it is interesting to consider that the above prediction be a semblance of the *average* of the ensemble. In this case, moving D14 up or down one unit in the sequence would not affect the composition of residues in the spanning domain on average, lending weight to the idea that a change in proton affinity due to depth rather than the hydrophobicity of the spanning segment is responsible for the altered pK_a we observed.

The corresponding spanning segment in R11Q;D14UpUp is the underlined portion of the sequence of the double variant: GGEQNPIYWAQDYAWLFTTPLLLLDLALLVDADEGTCG. It is interesting to see that moving the WT D14 up *two* units to position 12 brings it *outside* the putative frame, exchanging it for a tyrosine. This would result in an average hydrophobicity change of −1.14 kcal/mol (assuming a protonated aspartate), making the thermodynamics of the inserted segment more favorable, in agreement with the unexpected higher insertion pK_a we observed for R11Q;D14UpUp.

This concept of using simple hydrophobicity calculations of the putative spanning domain to predict the change in direction of the insertion pK_a correctly is something we have also done in other recent work[27] using membranes with different acyl chain lengths. In that other work, we found the MPEx results also to be good predictors of pHLIP's insertion pK_a in lipids with short to intermediate core thicknesses, leaving some hope that the semblance of an average may yet have practical use in our system.

■ ASSOCIATED CONTENT

Supporting Information

(1) Insertion reversibility experiments, (2) ionic and pH aggregation challenges, (3) comparative summary tables of CD and TF data, and (4) plots of TF spectral maxima vs pH for double variants. This material is available free of charge via the Internet at http://pubs.acs.org.

■ AUTHOR INFORMATION

Corresponding Author

*Address: Department of Molecular Biophysics and Biochemistry, Yale University, Bass Center, Room 425, 266 Whitney Ave., New Haven, CT 06511, USA. Telephone: +1 (203) 432-5600. E-mail: donald.engelman@yale.edu.

Funding

This work was supported by National Institutes of Health Grants R01-GM073857-04 and R01-CA133890-02.

Notes

The authors declare no competing financial interest.

■ ACKNOWLEDGMENTS

We thank Dr. Ming An, Dr. Damien Thevenin, Dr. Monika Musial-Siwek, Dr. Takemasa Kawashima, Dr. Miriam Alonso, Dr. Fred Gorelick, Dr. Michael Caplan, and Dr. Yorgo Modis for their time, support, and helpful discussions in the assembly of this work.

■ ABBREVIATIONS

pHLIP,pH low insertion peptide; CD,circular dichroism; TF,tryptophan fluorescence; LUV,large unilamellar vesicle; PET,positron emission tomography; HPLC,high-performance liquid chromatography; WT,wild type

■ REFERENCES

(1) Andreev, O. A., Dupuy, A. D., Segala, M., Sandugu, S., Serra, D. A., Chichester, C. O., Engelman, D. M., and Reshetnyak, Y. K. (2007) Mechanism and uses of a membrane peptide that targets tumors and other acidic tissues in vivo. *Proc. Natl. Acad. Sci. U.S.A. 104*, 7893−7898.

(2) Reshetnyak, Y. K., Andreev, O. A., Lehnert, U., and Engelman, D. M. (2006) Translocation of molecules into cells by pH-dependent insertion of a transmembrane helix. *Proc Natl Acad Sci U S A. 103*, 6460−6465.

(3) Thévenin, D., An, M., and Engelman, D. M. (2009) pHLIP-Mediated Translocation of Membrane-Impermeable Molecules into Cells. *Chem. Biol. 16*, 754−762.

(4) Reshetnyak, Y. K., Yao, L., Zheng, S., Kuznetsov, S., Engelman, D. M., and Andreev, O. A. (2011) Measuring Tumor Aggressiveness and Targeting Metastatic Lesions with Fluorescent pHLIP. *Mol. Imaging Biol. 13*, 1146−1156.

(5) Gillies, R. J., Raghunand, N., Garcia-Martin, M. L., and Gatenby, R. A. (2004) pH imaging. A review of pH measurement methods and applications in cancers. *IEEE Eng. Med. Biol. Mag. 23*, 57−64.

(6) Vavere, A. L., Biddlecombe, G. B., Spees, W. M., Garbow, J. R., Wijesinghe, D., Andreev, O. A., Engelman, D. M., Reshetnyak, Y. K., and Lewis, J. S. (2009) A novel technology for the imaging of acidic prostate tumors by positron emission tomography. *Cancer Res. 69*, 4510−4516.

(7) Segala, J., Engelman, D. M., Reshetnyak, Y. K., and Andreev, O. A. (2009) Accurate analysis of tumor margins using a fluorescent pH Low Insertion Peptide (pHLIP). *Int. J. Mol. Sci 10*, 3478−3487.

(8) An, M., Wijesinghe, D., Andreev, O. A., Reshetnyak, Y. K., and Engelman, D. M. (2010) pH-(low)-insertion-peptide (pHLIP) translocation of membrane impermeable phalloidin toxin inhibits cancer cell proliferation. *Proc. Natl. Acad. Sci. U.S.A. 107*, 20246−20250.

(9) Reshetnyak, Y. K., Segala, M., Andreev, O. A., and Engelman, D. M. (2007) A monomeric membrane peptide that lives in three worlds: in solution, attached to, and inserted across lipid bilayers. *Biophys. J. 93*, 2363−2372.

(10) Hunt, J. F., Rath, P., Rothschild, K. J., and Engelman, D. M. (1997) Spontaneous, pH-dependent membrane insertion of a transbilayer α-helix. *Biochemistry 36*, 15177−15192.

(11) Zoonens, M., Reshetnyak, Y. K., and Engelman, D. M. (2008) Bilayer interactions of pHLIP, a peptide that can deliver drugs and target tumors. *Biophys. J. 95*, 225−235.

(12) Reshetnyak, Y. K., Andreev, O. A., Segala, M., Markin, V. S., and Engelman, D. M. (2008) Energetics of peptide (pHLIP) binding to and folding across a lipid bilayer membrane. *Proc. Natl. Acad. Sci. U.S.A. 105*, 15340−15345.

(13) Barrera, F. N., Weerakkody, D., Anderson, M., Andreev, O. A., Reshetnyak, Y. K., and Engelman, D. M. (2011) Roles of Carboxyl Groups in the Transmembrane Insertion of Peptides. *J. Mol. Biol. 413*, 359−371.

(14) Andreev, O. A., Karabadzhak, A. G., Weerakkody, D., Andreev, G. O., Engelman, D. M., and Reshetnyak, Y. K. (2010) pH (low) insertion

peptide (pHLIP) inserts across a lipid bilayer as a helix and exits by a different path. *Proc. Natl. Acad. Sci. U.S.A. 107*, 4081−4086.
(15) White, S. H., and Wimley, W. C. (1999) Membrane protein folding and stability: Physical principles. *Annu. Rev. Biophys. Biomol. Struct. 28*, 319−365.
(16) Snider, C., Jayasinghe, S., Hristova, K., and White, S. H. (2009) MPEx: A tool for exploring membrane proteins. *Protein Sci. 18*, 2624−2628.
(17) Musical-Siwek, M., Karabadzhak, A., Andreev, O. A., Reshetnyak, Y. K., and Engelman, D. M. (2010) Tuning the insertion properties of pHLIP. *Biochim. Biophys. Acta 1798*, 1041−1046.
(18) Mehler, E. L., Fuxreiter, M., Simon, I., and Garcia-Moreno, E. B. (2002) The role of hydrophobic microenvironments in modulating pK_a shifts in proteins. *Proteins 48*, 283−292.
(19) Burstein, E. A., Abornev, S. M., and Reshetnyak, Y. K. (2001) Decomposition of protein tryptophan fluorescence spectra into log-normal components. I. Decomposition algorithms. *Biophys. J. 81*, 1699−1709.
(20) Ionescu, R. M., and Eftink, M. R. (1997) Global analysis of the acid-induced and urea-induced unfolding of staphylococcal nuclease and two of its variants. *Biochemistry 36*, 1129−1140.
(21) Kelly, S. M., and Price, N. C. (2000) The Use of Circular Dichroism in the Investigation of Protein Structure and Function. *Curr. Protein Pept. Sci. 1*, 349−384.
(22) Gawrisch, K., Gaede, H. C., Mihailescu, M., and White, S. H. (2007) Hydration of POPC bilayers studied by ^{1}H-PFG-MAS-NOESY and neutron diffraction. *Eur. Biophys. J. 36*, 281−291.
(23) Vostrikov, V. V., Hall, B. A., Greathouse, D. V., Koeppe, R. E., II, and Sansom, M. S. P. (2010) Changes in transmembrane helix alignment by arginine residues revealed by solid-state NMR experiments and coarse-grained MD simulations. *J. Am. Chem. Soc. 132*, 5803−5811.
(24) Killian, J. A., and von Heijne, G. (2000) How proteins adapt to a membrane−water interface. *Trends Biochem. Sci. 25*, 429−434.
(25) Caputo, G. A., and London, E. (2004) Position and ionization state of Asp in the core of membrane-inserted α-helices control both the equilibrium between transmembrane and nontransmembrane helix topography and transmembrane helix positioning. *Biochemistry 43*, 8794−8806.
(26) Lewis, B. A., and Engelman, D. M. (1983) Lipid bilayer thickness varies linearly with acyl chain length in fluid phosphatidylcholine vesicles. *J. Mol. Biol. 166*, 211−217.
(27) Barrera, F. N., Fendos, J. F., and Engelman, D. M. (2012) Membrane physical properties influence transmembrane helix formation. *Proc. Natl. Acad. Sci. U.S.A. 109*, 14422−14427.